A Novel Method to Improve the Accuracy of Torque Estimation for Robotic Joint with Harmonic Drive Transmission

Fei Yu, Shu Xiao, Minghong Zhu, and Zhenpeng Wang

***Abstract*—Joint torque feedback (JTF) is widely considered as an effective technique for improving the performance of robot control. To implement JTF technique to robot control schemes, it is essential to fully get the measurements or estimations of the output torque transmitted by the system. In previous research, output torque is commonly measured by joint built-in torque sensors which will change the robot joint mechanical structure, or through position encoder measurements with the transmission model of the joint. In this paper, a new filter method is adopted to improve the joint torque accuracy based on both precise model and position measurements. More specifically, an optimization method based on Unscented Kalman Filter (UKF) algorithm is used together with the harmonic drive compliance model to achieve higher output joint toque accuracy. The proposed method has been experimentally studied and its performance is compared with the measurements of a commercial torque sensor. And the results have verified the effectiveness of the proposed torque estimation method.**

***Index Terms*—joint torque feedback, harmonic drive compliance model, UKF, torque estimation**

I. Introduction

JOINT torque feedback (JTF) technique can be widely used to improve the performance of robot control in the field of robotics not only based on its effectiveness, but also its flexibility [1], [2]. The effect of the load torque could be greatly suppressed when JTF is adopted in the motion control of robot manipulators. In addition, JTF can ease the necessity of modeling the robot link dynamics. In most cases, joint torque sensing is used together as a valuable capability for robots. As robot joint is the basic unit of a robot control system, to make research of the robot joint characteristics and control is essential to fulfill the robot control missions. To satisfy the requirements of the movements and control of various kinds of robots [3], [4], it is quite important to implement JTF to robot control schemes for the use of robot joint torque estimations and compensations [5].

To implement JTF technique to robot control schemes in particular, there exist two popular methods to obtain the joint torque needed for feedback. One method is to equip torque sensors to the joint, which will certainly change the robot joint mechanical structure [6], [7]. Another method for estimating the joint torque that adopts harmonic drive transmission based on motor-side and link-side position measurements is proposed in this paper [8].

In previous research, the output torque is commonly obtained by sensors directly or by harmonic drive compliance mechanical model transmission. This method will have drawbacks in sensor accuracy and environment temperature disturbance, and the other will bring in time delay and low output torque accuracy. In [9], a new torque sensor with high sensitivity was proposed to resolve the trade-off characteristics of the sensitivity and the stiffness of torque sensors, and the key idea of this new sensor came from a 4-bar linkage shape which was proved to be useful to increase the sensitivity of the sensor 3.5 times without sacrificing the stiffness. Moreover, the first method that can be called built-in torque sensing also has a great cost of the force/torque sensor. So the second method provides a way to reduce the cost and also keep the robot joint mechanical structure properly.

For the second method, harmonic drive is adopted as the base of the whole transmission system. Due to the torsional compliance of the harmonic drive of which are wave generator, flexspline, and circular spline can be utilized for torque sensing, in recent years commercial high-resolution absolute position encoders are being applied in the harmonic drive transmission system. The encoders are mounted in motor-side and link-side respectively, and input and output position measurements are directly obtained to provide the elements needed for calculating the torsional torque. Then the torque can be used together with the harmonic drive compliance model to achieve output joint torque. This method has been proved effective to get similar torque precision compared with the built-in commercial sensors. Because of advantages, the harmonic drive based transmission is widely adopted and more research are being taken in this filed.

Torque estimation based on harmonic drive compliance model has been proved to be an economical and effective way for robotic joint torque estimation and control. As in [10], a link-side position encoder was adopted to measure the harmonic drive torsional deformation, which then was used together with the harmonic drive compliance model to estimate the joint torque. In [11], a harmonic drive built-in torque measuring method was proposed with a two-order ripple model to reduce the impacts of ripples, and proved to be effective to improve the torque accuracy. Reference [12] developed a dynamic model of the Mitsubishi PA-10 robot

Manuscript received March 17, 2018; revised September 2, 2018. This work was supported by the National Natural Science Foundation of China under Grant No. 51679047.

F. Yu is with the College of Automation, Harbin Engineering University, Harbin, 150001, China.

S. Xiao is with the College of Automation, Harbin Engineering University, Harbin, 150001, China (Corresponding author, e-mail: xiaoshu@hrbeu.edu.cn).

M. H. Zhu is with the College of Automation, Harbin Engineering University, Harbin, 150001, China (Corresponding author, e-mail: zhumh0109@163.com).

Z. P. Wang is with Sichuan Academy of Aerospace Technology, Chengdu, 610000, China.

arm for the purpose of implementing a low velocity trajectory tracking by using very low feedback gains, the novelty of which was to develop a new systematic algorithm to facilitate the robot control based on a harmonic drive transmission model.

In the joint torque estimation method of this paper, a new filter method is adopted to improve the joint torque estimation accuracy based on both precise model and position measurements [13] - [16]. More specifically, the dynamic model of the harmonic drive based joint setup is developed at the beginning. Based on the proposed dynamic model, torsional deformation model, and kinematic error model are developed to make compensations for the whole model. Then UKF technique is used together with the position measurements to estimate the output joint torque. It is a new method of making a torque estimation based on the whole system dynamic model, which effectively improves the accuracy of the output joint torque.

The rest of the paper is organized as follows. The dynamic model and estimation scheme of the harmonic drive based joint setup used in the experiments of this paper are presented in Section II. Based on the UKF technique, an optimization algorithm is derived in Section III. And the experiment results and final concluding remarks are given in Section IV and Section V, respectively.

II. Dynamic Model of the Harmonic Drive-Based Joint Setup

A. Kinematic Model of Harmonic Drive

The typical structure of a harmonic drive consists of three components: wave generator (WG), flexspline (FS), and circular spline (CS). A simple description: the wave generator is coupled with the motor shaft of a brushed DC motor through the plug of WG, the circular spline is connected to the joint housing, and the flexspline is sandwiched in between (CS and WG) and connected to the joint output side.

Fig. 1. The typical structure of a harmonic drive.

The specific structure of a harmonic drive is clearly shown in Fig. 1. The wave generator is a thin ball-bearing body which is matched into an elliptical plug. The flexspline is a thin cylinder cup-shaped structure with external teeth that are a bit smaller than the internal teeth of the circular spline [7]. To make them matching, the circular spline has rigid ring shape with the fitted external teeth. The operation principle of the harmonic drive can be explained briefly. As the wave generator rotates clockwise with the circular spline fixed, the flexspline is subjected to elastic deformation and its tooth engagement position moves turning relative to the circular spline. When the wave generator rotates 180 degrees clockwise, the flexspline moves counterclockwise by one tooth relative to the circular spline. For every one full rotation clockwise (360 degrees) of the wave generator, the flexspline moves counterclockwise by two teeth relative to the circular spline because the flexspline has two fewer teeth than there are on the circular spline. In general, this movement is treated as output power.

Based on the structure of the harmonic drive, the basic kinematic model of a harmonic drive can be represented in Fig. 2.

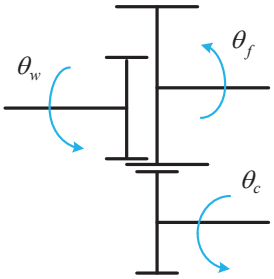

Fig. 2. The basic kinematic model of a harmonic drive.

The kinematic relationship of a harmonic drive can be explained below

$$\theta_w = (N+1)\theta_c - N\theta_f \tag{1}$$

wherein, N donates the gear ratio, θ_w, θ_f, and θ_c refer to the angular positions of the wave generator, flexspline, and circular spline, respectively. The above model is developed in the ideal condition of not considering the viscous friction and kinematic error due to gear meshing [17].

B. Dynamic Model of the Harmonic Drive-Based Joint Setup

To implement the harmonic drive transmission to a flexible joint, an experiment setup is developed as in Fig. 3.

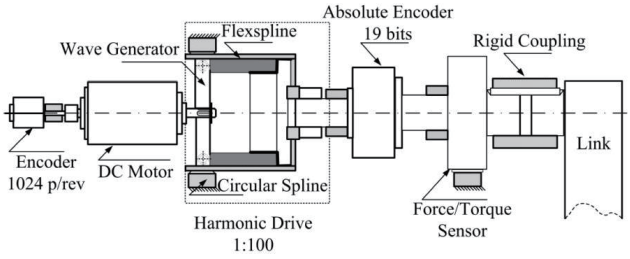

Fig. 3. The basic schematic model of the experiment setup.

The developed joint in this research is referred as test-joint. The DC motor is installed with an optical position encoder with 1024 p/rev to measure the motor angular displacement. On the link-side an absolute position encoder with 19 bits is mounted to measure the test-joint output angle. Motor input torque can be exerted by the motor input current.

When the joint friction and kinematic error are taken into consideration, the scheme illustration of the harmonic drive

compliance components can be expressed in Fig. 4. The specific parameters in the scheme will be given subsequently.

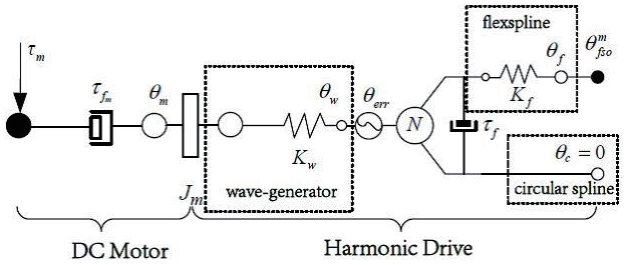

Fig. 4. Schematic illustration of the harmonic drive compliance.

Based on the scheme illustration of the harmonic drive, the dynamic model of the test setup with hysteresis effects can be described by the following differential equation:

$$J_m\ddot{\theta}_m + B_m\dot{\theta}_m + \tau_{fm} + \frac{\tau_f}{N} = \tau_m \tag{2}$$

wherein, θ_m, J_m, and B_m represent the position, rotary inertia, and damping factor on the motor side, respectively. τ_{fm} is the friction torque, τ_f represents the hysteresis torque which is treated as the output torque in the harmonic drive, and τ_m is the input motor torque which is proportional to the input current.

The system nonlinearity stems from three parts of the harmonic drive components: the torsional compliance, nonlinear friction forces, and kinematic error. The nonlinear kinematic relationship can be described by introducing compliance friction and kinematic error to the ideal kinematic model of the harmonic drive [18]. As shown in Fig. 4, θ_f and θ_w donate the link-side and motor-side angles, respectively. Zhang et al. in [8], proposed a model of the compliance of the harmonic drive components. When we assume $\Delta\theta$ as the total torsional angle of the harmonic drive, $\Delta\theta_f$ and $\Delta\theta_w$ are the torsional angles of the flexspline and the wave generator respectively, and θ_{err} is the kinematic error. Then the total torsional angle of the harmonic drive can be determined by

$$\Delta\theta = \Delta\theta_f + \frac{\Delta\theta_w}{N} + \theta_{err} \tag{3}$$

As the total torsional deformation model of the harmonic drive based joint setup has been discussed and the stiffness of the wave generator is considered above, we can get

$$\Delta\theta_f = \Delta\theta - \frac{\mathrm{sign}(\tau_w)}{C_w N K_w}(1 - e^{-C_w|\tau_w|}) - \theta_{err} \tag{4}$$

where C_w, N, and K_w are known parameters. τ_w can be calculated by the motor input torque, approximately.

The torsional angle $\Delta\theta_f$ of the flexspline is defined by the stiffness of the flexspline as

$$\Delta\theta_f = \frac{\arctan(C_f\tau_f)}{C_f K_f} \tag{5}$$

where C_f, K_f are known parameters.

The total torsional angle $\Delta\theta$ of the harmonic drive can be defined as

$$\Delta\theta = \theta_f - \frac{\theta_w}{N} \tag{6}$$

where θ_f, θ_w donate the link-side and motor-side angles, which can be measured by the encoders mounted on the motor and link side of the joint.

Kinematic error θ_{err} can be written as

$$\begin{aligned}\theta_{err} = {} & a_0 + a_{l1}\cos(\theta_f\omega_l) + b_{l1}\sin(\theta_f\omega_l) \\ & + a_{w1}\cos(\theta_w\omega_w) + b_{w1}\sin(\theta_w\omega_w) \\ & + a_{w2}\cos(2\theta_w\omega_w) + b_{w2}\sin(2\theta_w\omega_w)\end{aligned} \tag{7}$$

where the coefficients $a_0, a_{l1}, b_{l1}, \omega_l, a_{w1}, a_{w2}, b_{w1}, b_{w2}$, and ω_w are known parameters.

After acquiring the flexspline torsional deformation $\Delta\theta_f$, the joint torque estimation can be obtained by inverting (5) as

$$\tau_f = \frac{\tan(\Delta\theta_f C_f K_f)}{C_f} \tag{8}$$

One can use the compliance model (2) - (8) to estimate the joint torque. While it is mentioned in the literatures [8] - [10] that the maximum difference between the estimated torque and the torque sensor measurement is 1.825 N*m (about 36% of the maximum value of the total test torque), and the RMS level of the difference is 0.445 N*m about 10% of the maximum value of the total test torque. The poor accuracy limits the method to be used widely. To overcome the weaknesses of this compliance model, a new method based on UKF algorithm is used together with the harmonic drive compliance model to achieve higher output joint toque accuracy, and this will be described in the next part [19], [20].

III. A Torque Estimation Optimization Algorithm Based on UKF

The estimation results calculated from the previous model have proved that the single compliance model is unsuitable for widespread use for the implementation of the robotic joint control, because of the limitation of low torque estimation accuracy. To improve the situation and consider the dynamic model of the harmonic drive based joint setup, the torque estimation scheme can be developed in Fig. 5.

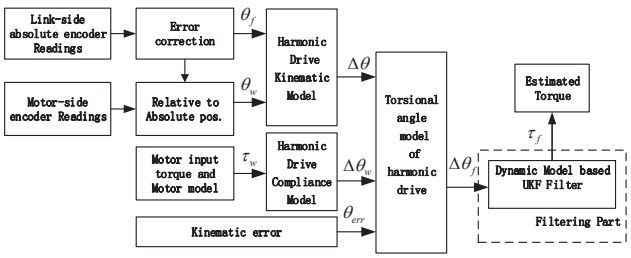

Fig. 5. Scheme of the torque estimation.

The new method of the torque estimation optimization algorithm based on both the harmonic drive dynamic model and UKF technique, can be expressed as below

$$X_k = f(X_{k-1}, u_{k-1}) + w_{k-1} \tag{9}$$

$$Z_k = h(X_k) + v_k \tag{10}$$

where $k \in N$, the state variable is $X = \begin{bmatrix} \dot{\theta}_m & \tau_f \end{bmatrix}^T$, and the measurement $Z = \begin{bmatrix} \dot{\theta}_m & \Delta\theta_f \end{bmatrix}^T$, can be got from the motor-side readings and calculated from the harmonic drive compliance model. X_k is the state variable of the system at time k, and Z_k is the measurement variable at time k. w_k and v_k are zero mean Gaussian white noise, Q_K and R_k are their covariance matrices, respectively.

Based on the compliance model from (2) - (8), $f(x)$ can be defined as

$$f(x)=F*X_{k-1}+B*u_{k-1} \tag{11}$$

where F and B can be obtained by the discrete model of (2), $u_{k-1}=\tau_m-\tau_{fm}$ represents the input, and $h(x)$ can be defined as

$$h(x)=\begin{bmatrix} X_{k-1}(1) & \arctan(X_{k-1}(2)*c_f)/(c_f*k_f) \end{bmatrix}^T \tag{12}$$

Then the optimization algorithm will run in the following form.

1) Initialize with :

$$\hat{X}_0=EX_0 \tag{13}$$

$$P_0=E[(X_0-\hat{X}_0)(X_0-\hat{X}_0)^T] \tag{14}$$

2) Calculate weights:

$$\begin{aligned} W_0^{(m)} &= \tfrac{\lambda}{n+\lambda} \\ W_0^{(c)} &= \tfrac{\lambda}{n+\lambda}+1-\alpha^2+\beta \\ W_i^{(m)} &= W_i^{(c)}=\tfrac{1}{2(n+\lambda)} \quad (i=1,2,\cdots 2n) \end{aligned} \tag{15}$$

where $\lambda=\alpha^2(n+\kappa)-n$, α is a very small positive number and $1e-4\le\alpha\le 1$; κ=3$-n$, β=2.

3) Calculate the sigma points at time k-1:

$$\tilde{\chi}_{k-1}^{(0)}=\hat{X}_{k-1} \tag{16}$$

$$\tilde{\chi}_{k-1}^{i}=\hat{X}_{k-1}+\gamma(\sqrt{P_{k-1}})_{(i)} \quad (i=1,2,\cdots n) \tag{17}$$

$$\tilde{\chi}_{k-1}^{i}=\hat{X}_{k-1}-\gamma(\sqrt{P_{k-1}})_{(i-n)} \quad (i=n+1,n+2,\cdots 2n) \tag{18}$$

4) State prediction: one-step state prediction and its covariance matrix at time k

$$\chi_{k/k-1}^{*(i)}=f[\tilde{\chi}_{k-1}^{i},u_{k-1}] \quad (i=1,2,\cdots n) \tag{19}$$

$$\hat{X}_{k/k-1}=\sum W_i^{(m)}\chi_{k/k-1}^{*(i)} \tag{20}$$

$$P_{k/k-1}=\sum W_i^{(c)}[\chi_{k/k-1}^{*(i)}-\hat{X}_{k/k-1}][\chi_{k/k-1}^{*(i)}-\hat{X}_{k/k-1}]^T+Q_{k-1} \tag{21}$$

5) Calculate one-step sample points prediction at time k:

$$\tilde{\chi}_{k/k-1}^{(0)}=\hat{X}_{k/k-1} \tag{22}$$

$$\tilde{\chi}_{k/k-1}^{i}=\hat{X}_{k/k-1}+\gamma(\sqrt{P_{k/k-1}})_{(i)} \quad (i=1,2,\cdots n) \tag{23}$$

$$\tilde{\chi}_{k/k-1}^{i}=\hat{X}_{k/k-1}-\gamma(\sqrt{P_{k/k-1}})_{(i-n)} (i=n+1,n+2,\cdots 2n) \tag{24}$$

6) Measurement update:

$$\overset{\approx}{Z}_{k/k-1}^{(i)}=h[\tilde{\chi}_{k/k-1}^{i}] \quad (i=0,1,2,\cdots 2n) \tag{25}$$

$$\hat{Z}_{k/k-1}=\sum W_i^{(m)}\overset{\approx}{Z}_{k/k-1}^{(i)} \tag{26}$$

$$P_{(XZ)_{k/k-1}}=\sum W_i^{(c)}[\chi_{k/k-1}^{(i)}-\hat{X}_{k/k-1}][\overset{\approx}{Z}_{k/k-1}^{(i)}-\hat{Z}_{k/k-1}]^T \tag{27}$$

$$P_{(ZZ)_{k/k-1}}=\sum W_i^{(c)}[\overset{\approx}{Z}_{k/k-1}^{(i)}-\hat{Z}_{k/k-1}][\overset{\approx}{Z}_{k/k-1}^{(i)}-\hat{Z}_{k/k-1}]^T+R_k \tag{28}$$

7) Estimation update: the filtering gain and the estimation of the state with its covariance matrix are

$$K_k=P_{(XZ)_{k/k-1}}{P^{-1}}_{(ZZ)_{k/k-1}} \tag{29}$$

$$\hat{X}_k=\hat{X}_{k/k-1}+K_k[Z_k-\hat{Z}_{k/k-1}] \tag{30}$$

$$P_k=P_{k/k-1}-K_kP_{(ZZ)_{k/k-1}}{K_k}^T \tag{31}$$

The whole torque estimation optimization algorithm based on UKF technique can be fully performed by (9) - (31). The algorithm is developed together with the dynamic model of the harmonic drive based joint setup, and the flexspline torsional deformation $\Delta\theta_f$ is added into the measurements to fulfill the process.

IV. Experiment Results

This section provides the experiment results of verifying the effectiveness of the proposed torque estimation optimization algorithm. An experiment system is set up as shown in Fig. 6. The Joint 1 in the figure is referred as test-joint, which is connected by a link-joint working as a robotic arm.

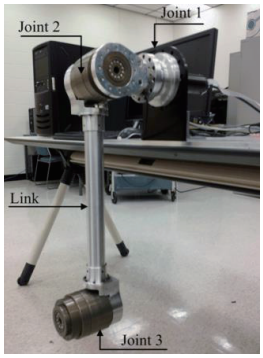

Fig. 6. The experiment joint setup.

The harmonic drive of the joint setup is driven by a brushed DC motor, which is coupled with a harmonic drive system of the model SHD-17-100-2SH with a gear ratio N=100, and the DC motor is instrumented with an optical incremental encoder to measure the motor angular displacement. On the link side a commercial ATI six-axis F/T sensor is used to measure the output torque of the test joint. Then the efficiency of the proposed torque estimation method is verified by comparing the estimated joint torque to the torque measurement from the F/T sensor mounted on the output side of the test-joint.

A. Experiment of Joint Based on the Compliance Model of the Harmonic Drive

This experiment of the joint is set with a gradually changing torque. And the joint is arranged to rotate in 58 seconds with a sinusoidal input. The experiment results only based on the compliance model of the harmonic drive have been

given in Fig. 7 and Fig. 8, including the torque estimation compared with a torque sensor and the difference.

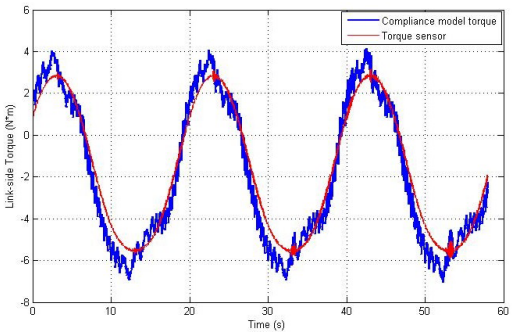

Fig. 7. Comparison between estimated torque based on compliance model and torque sensor.

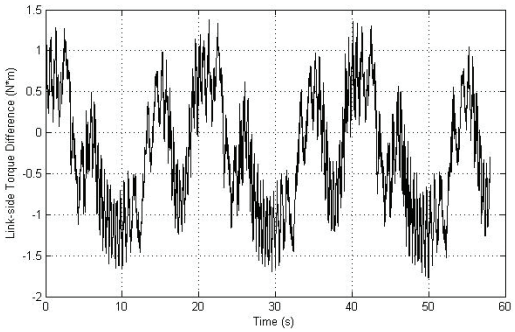

Fig. 8. Difference between estimation torque based on compliance model and torque sensor.

From Fig. 8, we get the maximum difference is 1.619 N*m which is about 30% of the maximum value of the test torque, and the RMS of the difference is 0.770 N*m (about 14.3% of the maximum value of the test torque).

B. Experiment of Joint Based on the Proposed Torque Estimation Optimization Algorithm

The joint test environment is set the same as in Section IV-A in which the joint is arranged to rotate in 58 seconds with a sinusoidal input. The experiment results based on the proposed torque estimation optimization algorithm have been given in Fig. 9 and Fig. 10, including the torque estimation compared with a torque sensor and the difference.

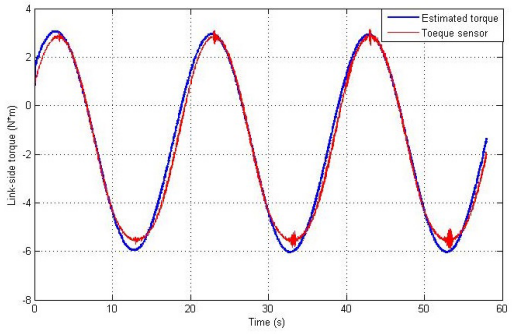

Fig. 9. Comparison between estimated torque based on proposed torque estimation optimization algorithm and torque sensor.

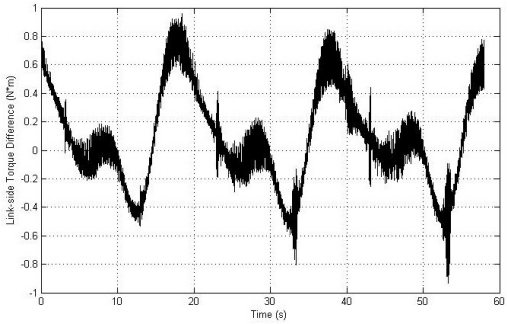

Fig. 10. Difference between estimated torque based on proposed torque estimation optimization algorithm and torque sensor.

From Fig. 10, we get the maximum difference is 0.922 N*m which is about 17% of the maximum value of the test torque, and the RMS of the difference is 0.350 N*m (about 6.5% of the maximum value of the test torque).

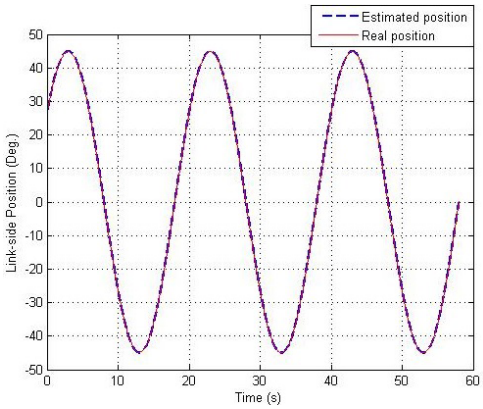

Fig. 11. Comparison between estimation position and real position.

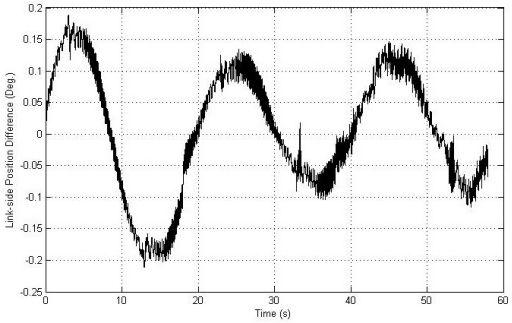

Fig. 12. Difference between estimation position and real position.

The real link-side position and it's estimated position are given in Fig. 11, the relative position error is shown in Fig. 12. From the two figures, we get the maximum position difference is 0.211 degrees which is quite small. So it is proved effective that the method can help to track the movement of the joint.

Based on the two experiments of the harmonic drive based joint setup, especially from Fig. 8 and Fig. 10, it is easy to see that the proposed method has helped to reduce the maximum torque difference from 1.619 N*m to 0.922 N*m, and the RMS of the difference from 0.770 N*m to 0.350 N*m. The results show 54.5% of the improvements of the estimated torque accuracy (based on the RMS of the difference).

V. Conclusion

In this paper, a new method to improve the accuracy of the torque estimation based on both the harmonic drive compliance model and UKF optimization algorithm is proposed. The harmonic drive compliance model is presented based on the components and physical characteristics of a harmonic drive, and the related torque estimation scheme is provided. After that, we develop the complete torque estimation optimization algorithm based on UKF technique. It is a new method of making a torque estimation based on the whole system dynamic model.

An experiment is set up with a gradually changing torque situation to verify the performance, in which the estimated torque is compared to a torque sensor measurement. And the results show that the proposed optimization algorithm based on UKF can bring 54.5% of the improvements of the estimated torque accuracy compared to torque estimation method which is only based on harmonic drive compliance model. The results have verified the effectiveness of the proposed torque estimation method. In the future, the proposed torque estimation method will be applied to more comprehensive research environment and motion control for promoting the method.

References

[1] F. Aghili, M. Buehler and J. M. Hollerbach, "Motion control systems with h-infinity positive joint torque feedback," *IEEE Trans. on Control Systems Technology*, vol.9, no.5, pp. 685-695, 2001.

[2] G. Liu, S. Abdul and A. Goldenberg, "Distributed modular and reconfigurable robot control with torque sensing," in *2006 IEEE Int. Conf. Mechatronics and Automation*, pp. 384-389.

[3] C. Rohrig, C. Kirsch, J. Lategahn and M. Muller, "Localization of autonomous mobile robots in a cellular transport system," *Engineering Letters*, vol.20, no.2, pp. 148-158, 2012.

[4] T. Taniguchi and M. Sugeno, "Trajectory tracking controls for non-holonomic systems using dynamic feedback linearization based on piecewise multi-linear models," *IAENG International Journal of Applied Mathematics*, vol.47, no.3, pp. 339-351, 2017.

[5] T. Kawakami, K. Ayusawa, H. Kaminaga and Y. Nakamura, "High-fidelity joint drive system by torque feedback control using high precision linear encoder," in *2010 IEEE Int. Conf. Robotics and Automation*, pp. 3904-3909.

[6] D. Tsetserukou, R. Tadakuma, H. Kajimoto and S. Tachi, "Optical torque sensors for implementation of local impedance control of the arm of humanoid robot," in *2006 IEEE Int. Conf. Robotics and Automation*, pp. 1674-1679.

[7] N. Kircanski, A. A. Goldenberg and S. Jia. "An experimental study of nonlinear stiffness, hysteresis, and friction effects in robot joints with harmonic drives and torque sensors," *International Journal of Robotics Research*, vol.16, no.2, pp. 214-239, 1997.

[8] H. Zhang, S. Ahmad and G. Liu, "Torque estimation technique of robotic joint with harmonic drive transmission," in *2013 IEEE Int. Conf. Robotics and Automation*, pp. 3034-3039.

[9] H. X. Zhang, Y. J. Ryoo and K. S. Byun, "Development of torque sensor with high sensitivity for joint of robot manipulator using 4-bar linkage shape," *Sensors*, vol.16, no.7, pp. 991, 2016.

[10] H. Zhang, S. Ahmad and G. Liu, "Torque estimation for robotic joint with harmonic drive transmission based on position measurements," *IEEE Trans. on Robotics*, vol.31, no.2, pp. 322-330, 2015.

[11] X. N. Pan, H. G. Wang and Y. Jiang, "A torque measuring method for robot joints with harmonic drives," *Advanced Materials Research*, pp. 694-697, 981-986, 2013.

[12] C. W. Kennedy and J. P. Desai, "Estimation and modeling of the harmonic drive transmission in the Mitsubishi PA-10 robot arm," in *2003 IEEE/RSJ Int. Conf. on Intelligent Robotots and Systems*, vol.3, pp. 3331-3336.

[13] K. Xiong, H. Zhang and L. Liu, "Adaptive robust extended Kalman filter for nonlinear stochastic systems," *Control Theory and Applications Iet*, vol.2, no.3, pp. 248-250, 2008.

[14] J. Seo, M. J. Yu, C. G. Park and J. G. Lee, "An extended robust $H\infty$ filter for nonlinear constrained uncertain systems," *IEEE Trans. on Signal Processing*, vol.54, no.11, pp. 4471-4475, 2006.

[15] C. A. Lightcap and S. A. Banks, "An extended Kalman filter for real-time estimation and control of a rigid-link flexible-joint manipulator," *IEEE Trans. on Control Systems Technology*, vol.18, no.1, pp. 91-103, 2010.

[16] A. Nattapol, "A bayesian filtering approach with time-frequency representation for corrupted dual tone multi frequency identification," *Engineering Letters*, vol.24, no.4, pp. 370-377, 2016.

[17] P. S. Gandhi and F. H. Ghorbel, "Closed-loop compensation of kinematic error in harmonic drives for precision control applications," *IEEE Trans. on Control Systems Technology*, vol.10, no.6, pp. 759-768, 2002.

[18] M. Ruderman, F. Hoffmann and T. Bertram, "Modeling and identification of elastic robot joints with hysteresis and backlash," *IEEE Transactions on Industrial Electronics*, vol.56, no.10, pp. 3840-3847, 2009.

[19] X. Chen, "An adaptive UKF-based particle filter for mobile robot S-LAM," in *Proc. 1st IITA International Joint Conf. Artificial Intelligence*, JCAI 2009, pp. 167-170.

[20] N. Edvard, H. H. I. King and B. Hannaford, "Robustness of the Unscented Kalman filter for state and parameter estimation in an elastic transmission," in *Proc. Robotics Science and Systems*, 2009.